Catalytic Properties of Supported MoO_3 Catalysts for Oxidative Dehydrogenation of Propane

Kaidong Chen, Enrique Iglesia and Alexis T. Bell

Chemical and Materials Sciences Divisions, Lawrence Berkeley National Laboratory, and Department of Chemical Engineering, University of California, Berkeley, CA 94720

The effects of MoO_x structure on propane oxidative dehydrogenation (ODH) rates and selectivity were examined on Al_2O_3-supported MoO_x catalysts with a wide range of surface density (0.4-12 Mo/nm^2), and compared with those obtained on MoO_x/ZrO_2. On MoO_x/Al_2O_3 catalysts, propane turnover rate increased with increasing Mo surface density and reached a maximum value for samples with ~ 4.5 Mo/nm^2. All MoO_x species are exposed at domain surfaces for Mo surface densities below 4.5 Mo/nm^2. Therefore, the observed trends reflect an increase in ODH turnover rates with increasing MoO_x surface density. As Mo surface densities increase above the polymolybdate monolayer value (~ 4.5 Mo/nm^2), ODH turnover rates decreased with increasing Mo surface density, as a result of the formation of MoO_3 crystallites with inaccessible MoO_x species. The ratio of rate constants (k_2/k_1) for propane combustion (k_2) and for propane ODH reactions (k_1) decreased with increasing MoO_x surface density and then remained constant for values above 5 Mo/nm^2. Propene combustion rate constants (k_3) also decreased relative to those for propane ODH (k_1) as two-dimensional structures formed with increasing Mo surface density. These Mo surface density effects on k_2/k_1 and k_3/k_1 ratios were similar on MoO_3/Al_2O_3 and MoO_3/ZrO_2, but the effects of Mo surface density on ODH turnover rates for samples with submonolayer MoO_x contents were opposite on the two catalysts. A comparison of ODH reaction rates and selectivity among MoO_3/Al_2O_3, MoO_3/ZrO_2, bulk MoO_3, $ZrMo_2O_8$, and $Al_2(MoO_4)_3$ suggests that the behavior of supported MoO_x at low surface densities resembles that for the corresponding bulk compounds ($ZrMo_2O_8$, and $Al_2(MoO_4)_3$), while at high surface density the behavior approaches that of bulk MoO_3 on both supports.

1. INTRODUCTION

Many recent studies have explored the oxidative dehydrogenation of light alkanes as a potential route to the corresponding alkenes. Oxidative dehydrogenation (ODH) of alkanes is favored thermodynamically and the presence of O_2 leads to the continuous removal of carbon deposits and to stable reaction rates. Secondary combustion reactions, however, limit alkene yields. For propane oxidative dehydrogenation reactions, the most active and selective catalysts are based on vanadium and molybdenum oxides [1-15]. On both V- and Mo-based catalysts, several studies of the kinetics and reaction mechanisms have shown that propane reactions occur via parallel and sequential oxidation steps (Scheme 1) [1-3, 11-14]. Propene forms via primary ODH reactions limited by the initial activation of the methylene C-H bond in propane (k_1), while CO and CO_2 (CO_x) can form via the combustion of the propene (k_3) formed in step 1 or the primary combustion of propane (k_2). The k_2/k_1 ratio (propane

combustion/propane dehydrogenation) is usually low (~0.1) for selective ODH catalysts [13-15]. The alkene yield losses observed with increasing conversion arise, for the most part, from large k_3/k_1 values (propene combustion/propane dehydrogenation ~ 10-50). These large k_3/k_1 values reflect the weaker allylic C-H bond in propene relative to the methylene C-H bond in propane and the higher binding energy of alkenes on oxide surfaces [12-15].

The structure and propane ODH catalytic properties of ZrO_2-supported MoO_3 catalysts were recently described [15]. Al_2O_3-supported MoO_3 catalysts have been widely used in hydrodesulfurization, hydrogenation, and alkene metathesis reactions, and detailed studies of the structure of dispersed MoO_3 on Al_2O_3 have been reported [16]. In contrast, little is known about the reaction pathways and the structural requirements for propane ODH reactions on MoO_x species supported on Al_2O_3 [8]. This work addresses the effect of Mo surface density on the propane ODH properties for MoO_3/Al_2O_3. The catalytic performance results obtained on MoO_3/Al_2O_3 were compared with those reported previously on MoO_3/ZrO_2.

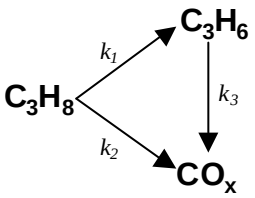

Scheme 1. Reaction network in oxidative dehydrogenation of propane

2. EXPERIMENTAL METHODS

Al_2O_3-supported MoO_x samples were prepared by incipient wetness impregnation of γ-Al_2O_3 (Degussa, AG) with a solution of ammonium heptamolybdate (AHM) (99%, Aldrich, Inc.) at a pH of 5. Impregnated samples were dried overnight in air at 393 K and then treated in dry air (Airgas, zero grade) at 773 K for 3 h. ZrO_2-supported MoO_x samples were also prepared by incipient wetness impregnation method, as described elsewhere [15].

Propane reaction rate and selectivity measurements were carried out at 703 K in a packed-bed tubular quartz reactor using 0.03-0.3 g samples. Propane (14 kPa; Airgas, 99.9%) and oxygen (1.7 kPa; Airgas, 99.999%) with He (Airgas, 99.999%) as a diluent were used as reactants. Reactants and products were analyzed by gas chromatography (Hewlett-Packard 5880 GC) using procedures described previously [13, 14]. C_3H_8 and O_2 conversions were varied by changing reactant space velocity (F/w; w: catalyst mass; F: reactant volumetric flow rate). Typical conversions were < 2% for C_3H_8 and < 20% for O_2. Initial ODH reaction rates and selectivities were obtained by extrapolation of these rate data to zero residence time. The effect of bed residence time on product yields was used in order to calculate rates and rate constants for secondary propene combustion reactions, using procedures reported previously [13, 14].

3. RESULTS AND DISCUSSION

The structures of MoO_3/Al_2O_3 and MoO_3/ZrO_2 catalysts were characterized by BET surface area measurements, X-ray diffraction, and Raman, UV-visible, and X-ray absorption spectroscopy in previous studies [15, 16]. These data showed that the structure and domain size of MoO_x species depend strongly on the Mo surface density and the temperature of treatment in air. For samples treated in dry air below 773 K and with Mo surface densities

below "monolayer" values (~4.5 Mo/nm^2), only two-dimensional MoO_x oligomers are detected on Al_2O_3 or ZrO_2 surface. As Mo surface densities exceed this monolayer coverage, crystalline MoO_3 forms. The size of the MoO_x domains increased gradually with increasing Mo surface density.

Propane ODH on Mo-based catalysts occurs via parallel and sequential oxidation pathways (Scheme 1) [15]. The reaction rate constants (k_1, k_2 and k_3) in Scheme 1 can be calculated from the effects of reactant residence time on propene selectivity [14]. Propene yields during propane ODH reactions depend on both k_2/k_1 and k_3/k_1; smaller values of either ratio lead to higher propene selectivity at a given propane conversion. Figure 1 shows the effects of Mo surface density on k_2/k_1 and k_3/k_1 values for MoO_3/Al_2O_3 catalysts. The value of k_2/k_1 reflects the relative rates of initial propane combustion and dehydrogenation. The values of k_2/k_1 decreased with increasing Mo surface density, until it reached a constant value of ~0.05 for surface densities above 5 Mo/nm^2 (Figure 1(a)). This gradual decrease in k_2/k_1 values with increasing MoO_x surface density suggests that Mo-O-Al sites or uncovered Al_2O_3 surfaces near MoO_x species catalyze the unselective conversion of propane to CO_x. This may reflect, in turn, the tendency of such sites to bind alkoxide intermediates more strongly than Mo-O-Mo structures in polymolybdate domains or on the surface of MoO_3 clusters. The complete coverage of Al_2O_3 surfaces by a polymolybdate monolayer leads to a high initial propene selectivity, which resembles that in samples with predominantly MoO_3 species. A similar decrease in k_2/k_1 with increasing surface density of the active oxide was reported previously on MoO_x/ZrO_2 [15] and VO_x/Al_2O_3 [13] catalysts.

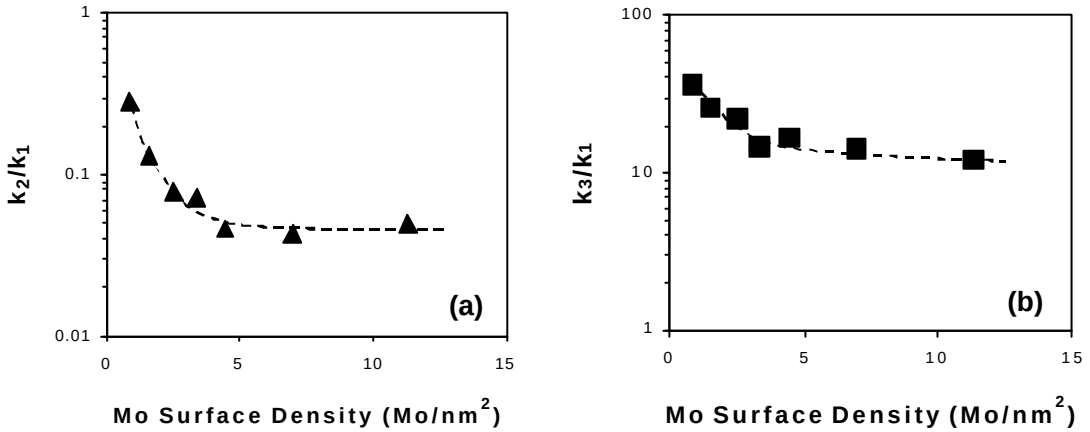

Fig. 1. Dependence of (a) k_2/k_1, and (b) k_3/k_1 on Mo surface density for MoO_x/Al_2O_3 [14 kPa C_3H_8, 1.7 kPa O_2, balance He, 703 K]

The values of k_3/k_1 were much greater than unity on all MoO_x/Al_2O_3 samples (Figure 1(b)), indicating that propene combustion occurs much more rapidly than propane dehydrogenation. It is this large value that causes the significant decrease in propene selectivity with increasing propane conversion. The values of k_3/k_1 (10-40) on these MoO_x/Al_2O_3 catalysts are similar to those measured on MoO_x/ZrO_2 [15]. The k_3/k_1 ratio decreased with increasing Mo surface density and then remained constant for Mo surface densities above 5 Mo/nm^2. The large k_3/k_1 ratio reflects the weaker C-H bonds in propene

compared to those in propane, as well as the higher binding energy of propene molecules on Lewis acid sites provided by Mo^{+6} cations present on MoO_3 surfaces [12].

Initial propane reaction rates are reported in Figure 2 as a function of Mo surface density on all MoO_x/Al_2O_3 samples. Propane consumption rates normalized per Mo atom initially increased with increasing Mo surface density and they approached maximum values at surface densities of ~ 4.5 Mo/nm^2 (Figure 2(a)). In this range of surface density, the accessibility of MoO_x at domain surfaces is largely unaffected by Mo surface density, because the Al_2O_3 surface is covered predominantly by two-dimensional MoO_x oligomers. Therefore, the observed increase in reaction rate reflects an increase in the reactivity (turnover rate) of exposed MoO_x active sites with increasing domain size. Propane reaction rates decreased as Mo surface densities exceed ~ 4.5 Mo/nm^2, which corresponds to the approximate surface density in a polymolybdate monolayer. The incipient appearance of three-dimensional MoO_3 structures, with the consequent incorporation of MoO_x into inaccessible positions within such clusters, is likely to account for the observed decrease in apparent turnover rates at higher surface densities (Figure 2(a)).

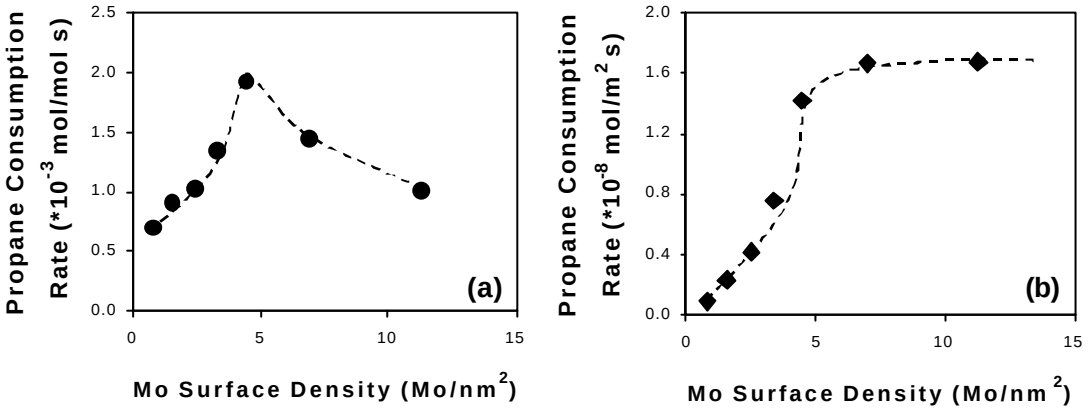

Fig. 2. Effects of Mo surface density on initial propane consumption rate for MoO_x/Al_2O_3 (a) normalized per Mo atoms, and (b) normalized per surface area. [14 kPa C_3H_8, 1.7 kPa O_2, balance He, 703 K]

Figure 2(b)shows the propane consumption rates normalized per BET surface area. These areal rates initially increased sharply with increasing Mo surface density, but then remained almost constant for surface densities above 5 Mo/nm^2. Thus, it appears that the initial increase in propane turnover rates as two-dimensional structures grow reflects the increasing reactivity of MoO_x surface structure on larger oxide domains. Similar domain size effects were observed on Al_2O_3-supported VO_x catalysts [13]. When Mo surface densities exceed monolayer coverages, three-dimensional MoO_3 form and the entire surface of the catalyst becomes covered by either two-dimensional MoO_x domains or MoO_3 clusters with similar surface reactivity. Any additional MoO_x species become inaccessible for propane ODH reactions; therefore, propane reaction rates normalized per Mo atom decreased, but areal rates remain constant with increasing MoO_x surface density.

The observed surface density effects on the catalytic activity of MoO_x/Al_2O_3 and MoO_x/ZrO_2 are different. On MoO_x/ZrO_2, propane turnover rates per Mo decreased with increasing Mo surface density, even below monolayer coverages [15]. Figure 3(a) compares

propane consumption rates per Mo atom on MoO_x/Al_2O_3 and MoO_x/ZrO_2. For Mo surface densities above ~ 5 Mo/nm^2, propane turnover rates on MoO_x/Al_2O_3 and MoO_x/ZrO_2 catalysts become similar, because in both cases catalyst surfaces are fully covered by two-dimensional or three-dimensional MoO_x species. Below monolayer coverages (~5 Mo/nm^2), however, propane turnover rates increased on MoO_x/Al_2O_3 but they decreased on MoO_x/ZrO_2 with increasing surface density.

Figure 3(b) shows the corresponding comparison for areal propane reaction rates on these two types of catalysts. Also shown in Figure 3(b) are areal rates on bulk $ZrMo_2O_8$, MoO_3 and $Al_2(MoO_4)_3$. It appears from these data that the catalytic activity of the surface structures in bulk $ZrMo_2O_8$ is considerable higher than on MoO_3 surfaces, which in turn, is higher than that on $Al_2(MoO_4)_3$ surfaces. This suggests that active species with surface structures similar to those on the surface of $ZrMo_2O_8$ may also be more active than those resembling the surfaces of bulk MoO_3, and more active still than those with surfaces resembling $Al_2(MoO_4)_3$. Since Mo surface densities in $ZrMo_2O_8$, MoO_3 and $Al_2(MoO_4)_3$ are similar, propane turnover rates would follow a sequence similar to that of the areal rates shown in Figure 3(b) ($ZrMo_2O_8$ > MoO_3 > $Al_2(MoO_4)_3$). For low surface density samples, the structures of MoO_x/Al_2O_3 and MoO_x/ZrO_2 surfaces would resemble those in the corresponding $Al_2(MoO_4)_3$ and $ZrMo_2O_8$ bulk phases. On MoO_x/Al_2O_3 catalysts, the surface structure gradually changes from one resembling $Al_2(MoO_4)_3$ to one similar to MoO_3 as the MoO_x surface density increases. Therefore, propane turnover rates increase with increasing Mo surface density for values below monolayer coverages, as surface structures evolve from isolated species with significant Mo-O-Al character to polymolybdate domains resembling in structure and in reactivity of the surface MoO_3 (Figure 3(a)). In contrast, the surface structure of MoO_x/ZrO_2 evolves from one resembling $ZrMo_2O_8$ to one similar to MoO_3 with increasing Mo surface density; as a result, propane turnover rates decrease with increasing Mo surface density (Figure 3(a)).

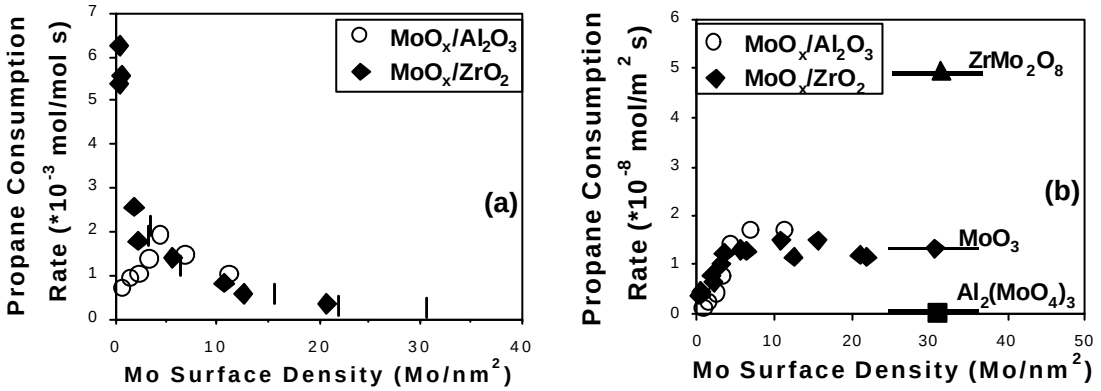

Fig. 3. Effects of Mo surface density on initial propane consumption rate on MoO_x/Al_2O_3, MoO_x/ZrO_2, bulk $ZrMo_2O_8$, MoO_3 and $Al_2(MoO_4)_3$. (a) normalized per Mo atoms, and (b) normalized per surface area. [14 kPa C_3H_8, 1.7 kPa O_2, balance He, 703 K].

Changes of k_2/k_1 and k_3/k_1 ratios as a function of Mo surface density on MoO_x/Al_2O_3 and MoO_x/ZrO_2 catalysts are consistent with the arguments presented above for the evolution of reaction rates with surface density on the two supports. Figure 4 shows k_2/k_1 and k_3/k_1 ratios on the supported MoO_x catalysts and on bulk $ZrMo_2O_8$, MoO_3 and $Al_2(MoO_4)_3$. The

k_2/k_1 and k_3/k_1 ratios on $Al_2(MoO_4)_3$ and on $ZrMo_2O_8$ are higher than on MoO_3. As Mo surface density increases, surface structures evolve from those resembling $Al_2(MoO_4)_3$ or $ZrMo_2O_8$ surfaces to MoO_3-like species; concurrently, k_2/k_1 and k_3/k_1 ratios decrease and approach those measured on MoO_3 (Figures 4(a) and 4(b)). These results suggest that at low surface densities, supported MoO_x species catalyze ODH reactions with turnover rates and selectivities strongly resembling those on the corresponding mixed oxide bulk structure.

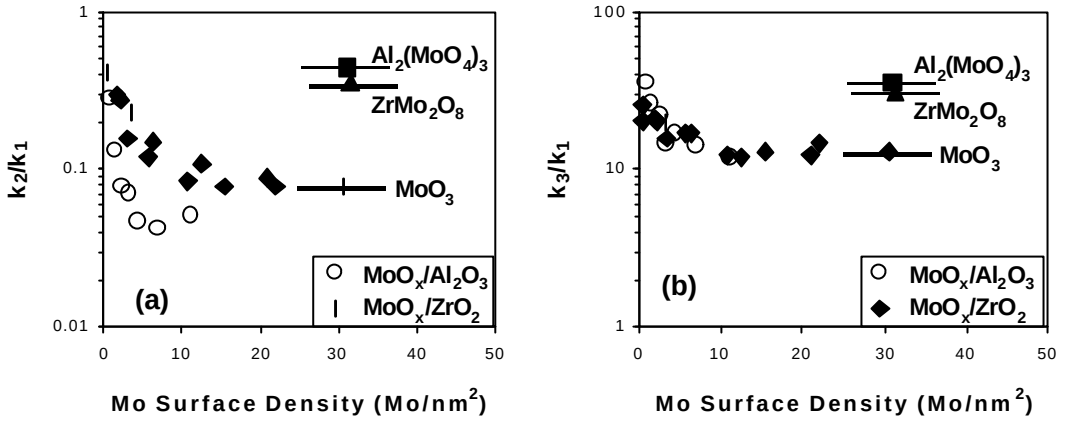

Fig. 4. Effects of Mo surface density on (a) k_2/k_1, and (b) k_3/k_1 ratio for MoO_x/Al_2O_3, MoO_x/ZrO_2, bulk $ZrMo_2O_8$, MoO_3 and $Al_2(MoO_4)_3$. [14 kPa C_3H_8, 1.7 kPa O_2, balance He, 703 K].

ACKNOWLEDGEMENT

This work was supported by the Director, Office of Basic Energy Sciences, Chemical Sciences Division of the U.S. Department of Energy under Contract DE-AC03-76SF00098.

REFERENCES

1. T. Blasko and J. M. López Nieto, Appl. Catal. A 157 (1997) 117.
2. H. H Kung, Adv. Catal. 40 (1994) 1.
3. S. Albonetti, F. Cavani and F. Trifiro, Catal. Rev. -Sci. Eng. 38 (1996) 413.
4. G. Centi and F. Triffiro, Appl. Catal. A 143 (1996) 3.
5. E. A. Mamedov and V. Cortés-Corberan, Appl. Catal. A 127 (1995) 1.
6. F. C. Meunier, A. Yasmeen and J. R. H. Ross, Catal. Today 37 (1997) 33.
7. L. E. Cadus, M. F. Gomez and M. C. Abello, Catal. Lett. 43 (1997) 229.
8. L. Jalowiecki-Duhamel, A. Ponchel and Y. Barbaux, J. Chim. Phys. PCB 94 (1997) 1975.
9. Y. S. Yoon, W. Ueda and Y. Moro-oka, Topics in Catal. 3 (1996) 256.
10. K. H. Lee, Y. S. Yoon, W. Ueda and Y. Moro-oka, Catal. Lett. 46 (1997) 267.
11. K. Chen, A. Khodakov, J. Yang, A. T. Bell and E. Iglesia, J. Catal. 186 (1999) 325.
12. K. Chen, A. T. Bell and E. Iglesia, J. Phys. Chem. B 104 (2000) 1292.
13. A. Khodakov, B. Olthof, A. T. Bell and E. Iglesia, J. Catal. 181 (1999) 205.
14. A. Khodakov, J. Yang, S. Su, E. Iglesia and A. T. Bell, J. Catal. 177 (1998) 343.
15. K. Chen, S. Xie, E. Iglesia and A. T. Bell, J. Catal. 189 (2000) 421.
16. K. Chen, S. Xie, A. T. Bell and E. Iglesia, J. Catal. in press.